DOI: 10.1002/anie.201107210

Protein-Based Force Probe

A Nanoscale Force Probe for Gauging Intermolecular Interactions**

*Minkyu Kim, Chien-Chung Wang, Fabrizio Benedetti, and Piotr E. Marszalek**

The development of single-molecule force spectroscopy (SMFS) techniques made it possible to probe the mechanical strength of covalent and non-covalent bonds mediating many interactions within biomolecular[1–4] and supramolecular systems.[5–8] Atomic force microscopy (AFM) measures the rupture force and extension of non-covalent bonds in interacting molecular systems, typically by attaching molecules of interest to the AFM tip and substrate through polymeric linkers such as poly(ethylene glycol) (PEG) that are connected to target molecules through, for example, thiol or amine coupling reactions.[4,8] However, the chemical complexity of proteins, which present multiple coupling targets, make the controlled chemical attachment of polymeric handles to specific points on molecular pairs quite challenging.

For SMFS of protein complexes, an alternative approach involves adding polypeptide handles at the DNA level.[9] In a recent approach, Bertz et al. elegantly created protein-based SMFS handles with a characteristic unfolding force ladder pattern to identify single-molecule experiments and accurately measure rupture events of protein homodimers.[9] This approach used rather strong reference protein modules and therefore is limited to protein complexes that separate at forces exceeding approximately 70 pN.[9] However, the strength of many biological interactions is expected to be less than 50 pN;[3,4,10–12] therefore, new force probes with higher force sensitivity are warranted.

To overcome this limitation, we report new protein-based handles and force probes for SMFS measurements of polypeptide pairs with a wide range of dissociation forces ($\geq$25 pN). The probe is composed of tandem repeats of the well-characterized protein module, the I27 domain of titin[13,14] and of staphylococcal nuclease (SNase),[15] I27-(SNase-I27)$_3$, as shown in Figure 1a and c. I27 domains mechanically unfold at approximately 200 pN and provide unmistakable single-molecule fingerprints in the form of a characteristic saw-tooth pattern which can be used to identify single-molecule recordings of new (uncharacterized) proteins.[16,17] SNase domains also produce a unique saw-tooth pattern but unfold at low forces of approximately 25 pN at the typical stretching speed of 200 nm s^{-1}.[15]

If the mechanical strength of a molecular complex to be studied is somewhat greater than 25 pN, then the SNase modules will unfold before the complex ruptures producing the unmistakable fingerprint of single-molecule measurements. If the molecular complex is stronger than 200 pN, then the force-extension curve will contain the mechanical fingerprints of SNase and I27. Thus, the use of SNase modules as a mechanical reference will allow the expansion of force spectroscopy measurements into low force regimes, allowing the examination of a wide range of weak biomolecular complexes.

We illustrate our approach using two systems: *Strep*-Tactin and *Strep*-tag II (Figure 1a) and ribonuclease (RNase) inhibitor and angiogenin (Figure 3a). The rupture force of the *Strep*-tag II/*Strep*-Tactin complex ($K_D \approx 1$ μM[18]) was estimated to be 40 pN.[12] The strength of the RNase inhibitor and angiogenin complex is presently unknown but is expected to be mechanically stronger than 40 pN based on the extremely low K_D (less than 1 fM[19]).

To examine the first system, we fused *Strep*-tag II into the C-terminus of our force probe. Then, *Strep*-tagged force probes were incubated with soluble *Strep*-Tactin, an engineered streptavidin with an increased *Strep*-tag binding affinity.[18] The mixture was deposited on a gold surface for SMFS measurements in solution.

Based on the design of our force probe (Figure 1a), we need to register a minimum of four regular SNase unfolding force peaks to be certain that the AFM tip picked up a fragment containing *Strep*-Tactin. Because *Strep*-Tactin tetramers provide four binding sites for *Strep*-tag II, each *Strep*-Tactin may have from zero up to four force probe molecules attached to it, generating several possible pulling geometries (see Supporting Information, Figure S1). However, the unique mechanical unfolding fingerprint of SNase modules allows us to identify the recordings obtained on individual versus multiple *Strep*-tag II/*Strep*-Tactin complexes (Figures S1 and S2). This approach circumvents the uncertainty as to the number of complexes (bonds) stretched which occurs when using soft polymeric linkers/handles, for which the force on a single complex (bond) is almost independent of the number of complexes (bonds) being stretched.[20]

Figure 1b illustrates an example of the AFM force-extension curve of *Strep*-tag II/*Strep*-Tactin complexes obtained using our force probe assay. The curve displays five regularly spaced unfolding force peaks (numbered 1–5).

[*] Dr. M. Kim, Prof. P. E. Marszalek
Center for Biologically Inspired Materials and Material Systems
Department of Mechanical Engineering and Materials Science
Duke University, Durham, NC 27708 (USA)
E-mail: pemar@duke.edu
Dr. C.-C. Wang
Graduate Institute of Biotechnology
National Chung-Hsing University, Taichung, Taiwan (R.O.C)
F. Benedetti
Laboratory of Physics of Living Matter, EPFL
Lausanne (Switzerland)

[**] We are grateful to Prof. J. Clarke (University of Cambridge, UK) for providing the pAFM 1–8 plasmid. We also thank Dr. J. Kim, Dr. M. Rabbi, and Z. Scholl for their help with the manuscript. This work was supported in part by National Institutes of Health grant GM079563 and National Science Foundation grant MCB-1052208.

Supporting information for this article is available on the WWW under http://dx.doi.org/10.1002/anie.201107210.

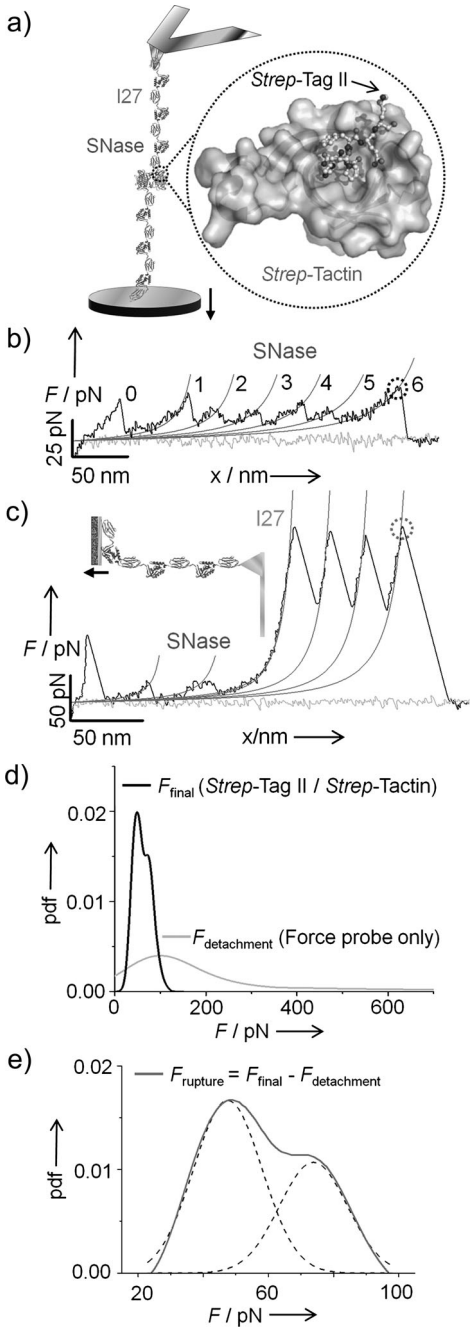

Figure 1. Design, characterization, and use of the protein-based force probe. a) A schematic of *Strep*-tagged force probes attached to the *Strep*-Tactin tetramer. In dotted circle, a schematic of *Strep*-Tactin monomer with a single *Strep*-tag II (PDB: 1KL5) is shown at higher magnification. b) A representative example of a force-extension curve of the *Strep*-tag II/*Strep*-Tactin complex linked to the force probes. Curves in (b) and (c) were obtained with the biolever AFM cantilever at a pulling speed of 200 nm s^{-1}. 0: A rupture of a nonspecific adhesion bond. 1–5: The unfolding of five individual SNase modules stretched in a WLC manner. 6: A final force peak obtained with the force probe on the *Strep*-tag II/*Strep*-Tactin complex. Thin gray solid lines on force curves are WLC fits with average contour length increments, $\Delta L_c = 46$ nm, and the persistent length, $p = 0.7$ nm. c) An example of a force-extension curve of the molecular force probe alone that captures the detachment event (gray dashed circle). Thin gray solid lines are WLC model fits to the curve with average $\Delta L_c = 46$ nm (SNase) and 29 nm (I27), and $p = 0.6$ nm (SNase) and 0.5 nm (I27). d) The comparison of the pdfs of final force peaks obtained from *Strep*-tag II/*Strep*-Tactin complexes (black solid line, $n = 96$) and force probes alone (gray solid line, $n = 113$). Data were collected with the microlever AFM cantilever at the pulling speed of 1000 nm s^{-1}. e) The pdf of rupture forces on the *Strep*-tag II/*Strep*-Tactin complex (dark gray solid line).

Fitting the worm-like chain (WLC) model to the data indicates that each unfolding event contributes 46 nm to the length of the polypeptide chain, which is consistent with the structure of SNase.[15] Moreover, these unfolding forces are identical to the unfolding forces of SNase in SNase-I27 force probe alone (Figure 1c and Figure S3). Furthermore, we note that when stretching the *Strep*-tag II and *Strep*-Tactin complex, we never recorded I27 unfolding force peaks in those experiments which captured four or more SNase unfolding force peaks. However, I27 unfolding force peaks were readily recorded together with SNase unfolding force peaks in control experiments when we stretched force probes alone (without *Strep*-Tactin, Figure 1c). These observations provide strong evidence that the AFM force curve in Figure 1b was obtained on individual complexes as illustrated in Figure 1a.

The final force peak in Figure 1b (peak 6, marked by a black dashed circle), which is followed by a sudden drop of force to zero, indicates that the molecular bridge between the AFM tip and the substrate broke because: either *Strep*-tag II was separated from *Strep*-Tactin or one of the handles detached from the tip or the substrate. To distinguish between these two possibilities, we measured the detachment forces separately by using only *Strep*-tagged force probes without *Strep*-Tactin (Figure 1c).

We determined the probability density function (pdf) of the last force peaks from the force curves obtained on the *Strep*-tag II and *Strep*-Tactin complexes. Then, the pdf obtained from the complex is compared with the pdf of detachment forces (Figure 1d; the respective histograms are shown in Figure S4). While the distribution of detachment forces is wide and extends beyond 700 pN, the distribution of final force peaks of the complex is narrow and centered around 60 pN, which is comparable to the 40 pN dissociation force determined for this system by AFM measurements reported in reference [12]. We conclude that the majority of final force peaks (> 70%) illustrated in Figure 1b report rupture events of the complex and not detachment events.

Surprisingly, subtracting the pdf of detachment forces from the pdf of final rupture forces produces the distribution (Figure 1e) that needs to be fitted with two Gaussians rather than one. The first maximum occurs at 48 ± 10 pN (mean $\pm$ standard deviation) and the second at 74 ± 10 pN. Since, in our assay, we only probe the strength of individual *Strep*-Tag II/*Strep*-Tactin complexes (Figure 1a), the two types of rupture events revealed by these pdfs cannot be explained by including events involving multiple complexes (Figure S1b–d). To clarify this result, we examined the unbinding forces between *Strep*-tag II/*Strep*-Tactin at different loading rates[3,4] varying between 50 pN s^{-1} and 7000 pN s^{-1}. We found that all distributions of rupture forces need to be fitted with

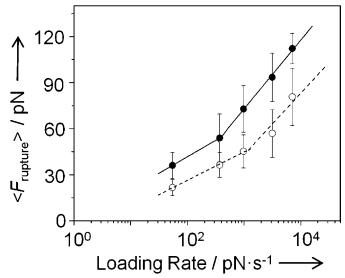

Figure 2. Dependence of the *Strep*-tag II/*Strep*-Tactin average rupture forces, $\langle F_{rupture}\rangle$, on the loading rates. Filled circles mark $\langle F_{rupture\text{-}high}\rangle$ and open circles mark $\langle F_{rupture\text{-}low}\rangle$. Error bars represent standard deviation.

two Gaussians that peak at $\langle F_{rupture\text{-}low}\rangle$ and $\langle F_{rupture\text{-}high}\rangle$ (Figure 2; Supporting Information). Similar to streptavidin–biotin complexes,[3] we found two linear regions with different slopes for both $\langle F_{rupture}\rangle$ when plotted against the loading rate (Figure 2). This observation suggests a complicated energy landscape of the *Strep*-tag II/*Strep*-Tactin complex with multiple energy barriers.[3]

We interpret these results as indicative of two distinct rupture pathways. These pathways may result from different pulling geometries and molecular configurations (Figure S6). We hypothesize that high rupture forces, $\langle F_{rupture\text{-}high}\rangle$, are measured when *Strep*-tag ligands are removed from monomers belonging to one *Strep*-Tactin dimer and low rupture forces, $\langle F_{rupture\text{-}low}\rangle$, are measured when *Strep*-tag ligands are bound to two different dimers within the same *Strep*-Tactin tetramer (for details, see the Supporting Information). Based on our recent study of streptavidin tetramers,[21] it is also possible that some of the rupture forces measured here may actually represent the forced separation of *Strep*-Tactin dimers from each other and not unbinding *Strep*-tag ligands. This hypothesis will be further tested by connecting our force probes directly to *Strep*-Tactin monomers (at the DNA level) and measuring the mechanical strength of the association of *Strep*-Tactin monomers within tetramers.

In a similar manner to construct *Strep*-tagged force probe, the RNase inhibitor and the angiogenin are also genetically fused into the C-terminus of the force probe. Then, the I27-(SNase-I27)$_3$-RNase inhibitor and I27-(SNase-I27)$_3$-angiogenin proteins are pre-incubated together to create RNase inhibitor/angiogenin complexes (Figure 3a).

Figure 3b represents an example of an AFM-obtained force-extension curve of RNase inhibitor/angiogenin complex using the force probe. By counting the number of regularly spaced SNase unfolding force peaks on the curve, we can easily identify that the complex was being stretched as illustrated in the inset of Figure 3b. Moreover, we note that the maximum forces to rupture the complex are equivalent or less than the unfolding force of an I27 module because maximum force peaks with four (or more) SNase unfolding force peaks were mostly followed by the unfolding force peak of only a single I27 domain (Figure 3b).

The final force peaks obtained on the RNase inhibitor/angiogenin complexes are distributed up to around 200 pN, while the distribution of detachment events is wider and

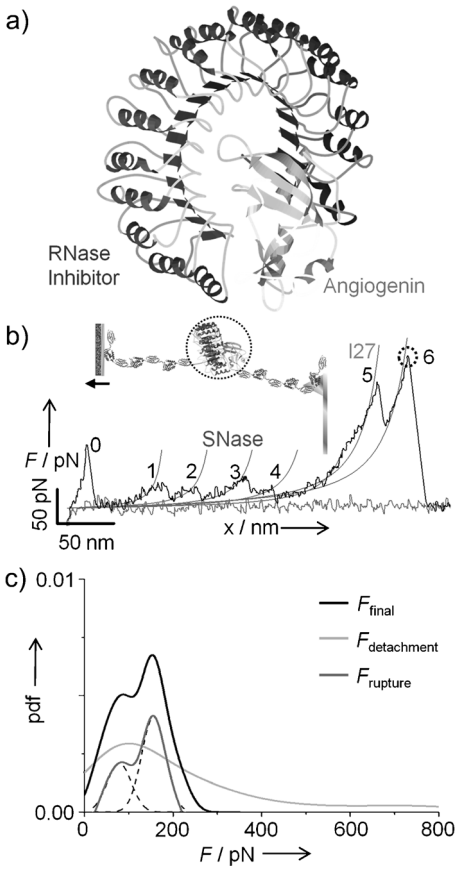

Figure 3. Measuring the intermolecular strength between the RNase inhibitor and angiogenin by AFM-based force probe assay. a) A schematic of the RNase inhibitor/angiogenin complex (PDB: 1A4Y). b) An example of a force-extension curve of the RNase inhibitor/angiogenin complex connected to the force probes. 0: A rupture of a nonspecific adhesion bond. 1–4: The unfolding of four individual SNase modules. 5: The unfolding of a single I27 domain. 6: A final force peak. WLC fits (thin solid gray lines) to the data represent average $\Delta L_c = 47$ nm and $p = 0.7$ nm (SNase), and $\Delta L_c = 29.5$ nm and $p = 0.35$ nm (I27). c) The comparison of the pdfs obtained based on the final force peaks from the complex (black solid line, $n = 68$) and detachment forces of I27-(SNase-I27)$_3$ constructs without the complex (gray dashed circle in Figure 1c; gray solid line, $n = 108$). The pdf of rupture forces on the complex (dark gray solid line) was determined by the same way as shown in Figure 1e. The curve in (b) and data in (c) were collected with the microlever AFM cantilever at the pulling speed of 500 nm s^{-1}.

extends beyond 800 pN (Figure 3c; the respective histograms are shown in Figure S8). In order to distinguish the rupture events between RNase inhibitor and angiogenin, the pdf of detachment forces was subtracted from the pdf of final rupture forces in the same way as shown in Figure 1e. Interestingly, the distribution of rupture events (the dark gray solid line in Figure 3c) was necessary to be fitted by two Gaussians with the first maximal force of 78 ± 27 pN and the next of 156 ± 27 pN. These two rupture forces of the RNase inhibitor/angiogenin complex can be explained by a two-step binding mechanism.[19] It has been reported that the RNase inhibitor and angiogenin may undergo conformational selection by first forming a loosely bound complex with K_D of

0.5 μM, and then immediately forming a tight complex with K_D of 0.7 fM.[19] Therefore, the two distributions that we observed possibly reflect the rupture forces of the weak and tight complexes with different binding affinities of RNase inhibitor/angiogenin complexes.

We note that, in specific systems examined here, I27 domains were not used for fingerprinting single-molecule rupture events but were very useful in measurements of detachment forces. When probing molecular complexes with higher affinities that will likely rupture at greater forces exceeding the unfolding force of I27, the presence of both mechanically weak and strong reference modules will be advantageous.[21]

So far, we demonstrated the use of our force probe to measure single rupture events involving two polypeptide components in an "A–B–A" and "A–B" configuration. By genetically fusing protein "C" to our force probe, we can similarly examine by AFM "A–B–C" (also "A–A") configurations, allowing us to reliably probe the strength of interactions within numerous protein complexes composed of homo- and hetero-dimers, and even higher oligomeric forms.

Received: October 12, 2011
Revised: December 16, 2011
Published online: January 17, 2012

Keywords: bond rupture measurements · ligand–receptor interactions · protein engineering · protein–protein interactions · single-molecule force spectroscopy

[1] J. Liang, J. M. Fernandez, *ACS Nano* **2009**, *3*, 1628 – 1645.
[2] E. M. Puchner, H. E. Gaub, *Curr. Opin. Struct. Biol.* **2009**, *19*, 605 – 614.
[3] E. Evans, *Annu. Rev. Biophs. Biomol.* **2001**, *30*, 105 – 128.
[4] P. Hinterdorfer, A. Ebner, H. Gruber, R. Kapon, Z. Reich in *Handbook of Nanotechnology*, 3rd ed. (Ed.: B. Bhushan), Springer, Heidelberg, **2010**, pp. 763 – 785.
[5] T. Hugel, M. Seitz, *Macromol. Rapid Commun.* **2001**, *22*, 989 – 1016.
[6] P. Samori, *Chem. Soc. Rev.* **2005**, *34*, 551 – 561.
[7] S. Zou, H. Schonherr, G. J. Vancso, *Angew. Chem.* **2005**, *117*, 978 – 981; *Angew. Chem. Int. Ed.* **2005**, *44*, 956 – 959.
[8] F. R. Kersey, W. C. Yount, S. L. Craig, *J. Am. Chem. Soc.* **2006**, *128*, 3886 – 3887.
[9] M. Bertz, J. Chen, M. J. Feige, T. M. Franzmann, J. Buchner, M. Rief, *J. Mol. Biol.* **2010**, *400*, 1046 – 1056.
[10] A. Janshoff, M. Neitzert, Y. Oberdorfer, H. Fuchs, *Angew. Chem.* **2000**, *112*, 3346 – 3374; *Angew. Chem. Int. Ed.* **2000**, *39*, 3212 – 3237.
[11] V. Dupres, C. Verbelen, Y. F. Dufrene, *Biomaterials* **2007**, *28*, 2393 – 2402.
[12] J. L. Tang, A. Ebner, H. Badelt-Lichtblau, C. Völlenkle, C. Rankl, B. Kraxberger, M. Leitner, L. Wildling, H. J. Gruber, U. B. Sleytr, N. Ilk, P. Hinterdorfer, *Nano Lett.* **2008**, *8*, 4312 – 4319.
[13] M. Rief, M. Gautel, F. Oesterhelt, J. M. Fernandez, H. E. Gaub, *Science* **1997**, *276*, 1109 – 1112.
[14] M. Carrion-Vazquez, A. F. Oberhauser, S. B. Fowler, P. E. Marszalek, S. E. Broedel, J. Clarke, J. M. Fernandez, *Proc. Natl. Acad. Sci. USA* **1999**, *96*, 3694 – 3699.
[15] C.-C. Wang, T.-Y. Tsong, Y.-H. Hsu, P. E. Marszalek, *Biophys. J.* **2011**, *100*, 1094 – 1099.
[16] H. B. Li, W. A. Linke, A. F. Oberhauser, M. Carrion-Vazquez, J. G. Kerkviliet, H. Lu, P. E. Marszalek, J. M. Fernandez, *Nature* **2002**, *418*, 998 – 1002.
[17] J. P. Junker, F. Ziegler, M. Rief, *Science* **2009**, *323*, 633 – 637.
[18] I. P. Korndorfer, A. Skerra, *Protein Sci.* **2002**, *11*, 883 – 893.
[19] K. A. Dickson, M. C. Haigis, R. T. Raines, *Prog. Nucleic Acid Res.* **2005**, *80*, 349 – 374.
[20] U. Seifert, *Phys. Rev. Lett.* **2000**, *84*, 2750 – 2753.
[21] M. Kim, C.-C. Wang, F. Benedetti, M. Rabbi, V. Bennett, P. E. Marszalek, *Adv. Mater.* **2011**, *23*, 5684 – 5688.

